FINITE ELEMENT ANALYSIS OF CROSS-HALVED JOINTS FOR STRUCTURAL COMPOSITES

Elemer M. Lang†

Assistant Professor
Division of Forestry
West Virginia University
Morgantown, WV 26506

and

Tamas Fodor

Associate Professor
Department of Technical Mechanics
University of West Hungary
Sopron, Hungary

ABSTRACT

The strength and stiffness of a notched, cross-halved joint was investigated using a three-dimensional finite element method (FEM). Composites involved in this research were laminated veneer lumber (LVL) and laminated strand lumber (LSL). The joint consisted of primary and secondary load-carrying elements notched and inserted into each other crosswise. A 3-D FEM technique predicted the deformations and stress developments under concentrated and distributed loads. Experimental validation of the model, based on deformation measurements, showed good to excellent agreement between predicted and measured values. Failure mode analysis revealed that the normal stresses (tension) control the performance of the joint.

The joint configuration can provide additional lateral stiffness and stability in structural applications including floor and roof systems. Furthermore, the in-plane moment resistance of the joint may provide better performance of such structures under dynamic loads such as earthquakes and excessive wind loads.

Keywords: Wood-based structural composites, FEM, stress, deformation, joint.

INTRODUCTION

As a major construction material supplier, the wood-based composite industry is under constant pressure to meet increasing demand using decreasing quantity and quality of material resources. New products such as oriented strandboard (OSB), laminated veneer lumber (LVL), parallel strand lumber (PSL), and laminated strand lumber (LSL) have been developed to meet demands of the construction industry. Besides "engineering out" the natural defects and inherent inconsistencies of solid wood, these products use short rotation trees and species previously neglected because of unfavorable physical and mechanical properties.

Although the wood-based composite industry has aided better utilization of resources, there is still potential to decrease the volume of wood in residential and commercial structures. Traditionally, load-bearing, structural composites were developed to replace solid wood in structural applications. Thus, the *in situ* usage is similar to that developed for lumber hundreds of years ago. The improved and more predictable engineering properties of these materials permit engineers to design lighter and more innovative structures that offer better performance.

For structural applications, a reticulated lat-

† Member of SWST.

tice structure, built with combinations of several types of wood composites, is envisioned. The proposed structure consists of two elements, primary load-bearing members and load-transferring members. The width of the members is aligned perpendicular to the principal plane. Halving joints connect the elements without any fasteners or gluing. Figure 1a shows the constructional principle of the proposed structure. The short, load-transferring members provide lateral support for the slender load bearing beams. With appropriate spacing and systematically shifted load-transferring elements, different lattice structures could be created including flat grids or hyperbolic shells as shown in Figs. 1b and 1c, respectively. Upon loading, the joints at the nodal points of the lattice become self-locking, owing to the joint configuration. This action provides both in-plane and vertical strength and stiffness. The symmetric structure of the lattice allows the use of advanced engineering techniques, like matrix structural analysis and finite element modeling, to dimension the members and optimize the spacing.

There are two major concerns regarding the final performance of such systems. Wood and wood-based composites are hygroscopic materials that shrink and swell according to their fluctuating moisture content. The subsequent dimensional changes, mainly in the thickness direction, can alter the tightness of the joint, creating difficulties in assembly and/or generating additional stresses during service. While the precision problem can be handled by notching the element in controlled environment, the effect of *in situ* shrinkage or swelling on the system should be investigated on full-scale assemblies in changing environmental conditions. Another consideration is the overall system behavior. The performance of a single joint may be modeled with reasonable accuracy. However, due to the cumulative effect of any discrepancies at the individual elements (joints), the global analysis may be seriously impaired as demonstrated by other researchers (ASCE 1976; Li and Schmidt 1997). All the same, it is assumed that the strength
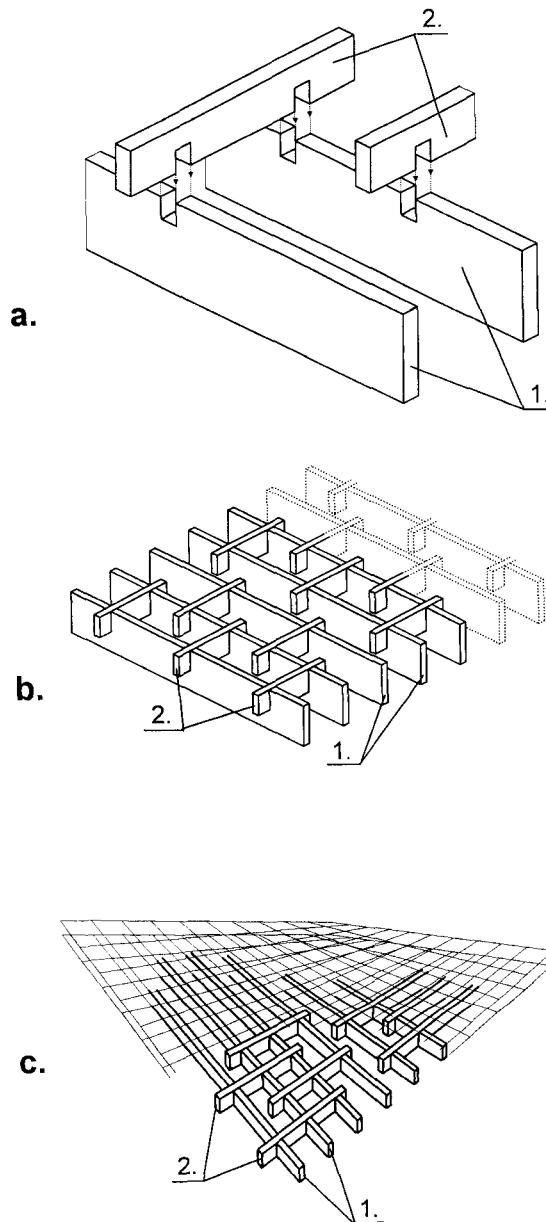

Fig. 1. The principle of the proposed joint system and two possible applications. 1.—Primary load-bearing elements; 2.—Load transferring elements.

and stiffness of the joints (i.e., material adequacy) can be explored using finite element modeling. The general load-supporting capacity of a lattice structure can be further evaluated by either modifying the local model or by structural matrix analysis.

BACKGROUND

Strength and stiffness of notched, solid wood beams have been intensively investigated in the past. Stieda (1966) studied the stress concentrations around holes and notches and their effect on the strength of wood beams. Murphy (1986) studied the strength and stiffness reduction of large notched beams. Zalph and McLain (1992) used a critical filet hoop stress model for predicting the failure loads of notched beams. Design equations were developed by Foliente and McLain (1992a) to better approximate the load-supporting capacity of end-notched beams. A finite element model was presented by Foliente and McLain (1992b) for predicting the strength of end-notched wood beams. Although the structure analyzed in the present study had no unfilled notches, the above-mentioned works provide vital information regarding stress concentrations, failure modes, and design approaches.

Goodman et al. (1974) investigated the composite and two-way actions in wood joist floor systems. They concluded that the ply-wood sub-flooring fixed to the joists significantly improved the strength and stiffness of the entire system. The additional lateral stiffening by the load-transferring element in the proposed structure may further improve the stability and load-supporting capacity of light frame buildings.

Other possible applications of the proposed joint include reticulated shells and lattice domes. Such structures were studied intensively over the past two decades. A Task Committee of the American Society of Civil Engineers presented a comprehensive review of lattice structures (ASCE 1976). In this work the historical development, analyses of lattice structures, and design practices are discussed. The authors pointed out the importance and economic significance of the non-planar joints in the framework.

Most of the numerous publications addressed the analysis, stability, and design of reticulated lattice structures created from rolled, extruded, or tubular metal elements.

However, fewer works targeted the performance of wood composites in complex systems. The most comprehensive paper was published by Holzer et al. (1991). The authors reviewed different stability investigations of spatial wood structures.

Several research projects conducted on reticulated load-bearing systems were initiated in Japan, where the imminent danger of earthquakes requires lightweight and ductile building constructions. Yamada (1989) evaluated the effects of joint flexibility and loading conditions on the buckling characteristics of latticed domes. Takashima (1993) developed a numerical simulation of elasto-plastic behavior of reticulated domes. Suzuki et al. (1994) proposed a woven lattice, shell structure made of flat steel bars and investigated the mechanical properties by means of analytical and experimental methods. Results indicated the superior load supporting capabilities of such structures.

OBJECTIVES

The ultimate goal of this research is to develop a fully engineered, lightweight, unique load-supporting system for residential and commercial building constructions and other applications. The primary goal of the present work was to confirm that notched, structural composite lumbers could support significant loads. Furthermore, the investigation focused on the stress concentration and distribution patterns around the critical areas of the proposed joint demonstrating the applicability of finite element analysis to wood-based composite materials. Specific objectives of this phase of the research were as follows:

1. To explore the engineering properties of the composites that govern the structural behavior of the proposed joint;
2. To develop a database of engineering properties of the materials for future use by standard testing procedures;
3. To develop analytical methods for predicting the behavior of the proposed joint via finite element modeling and;
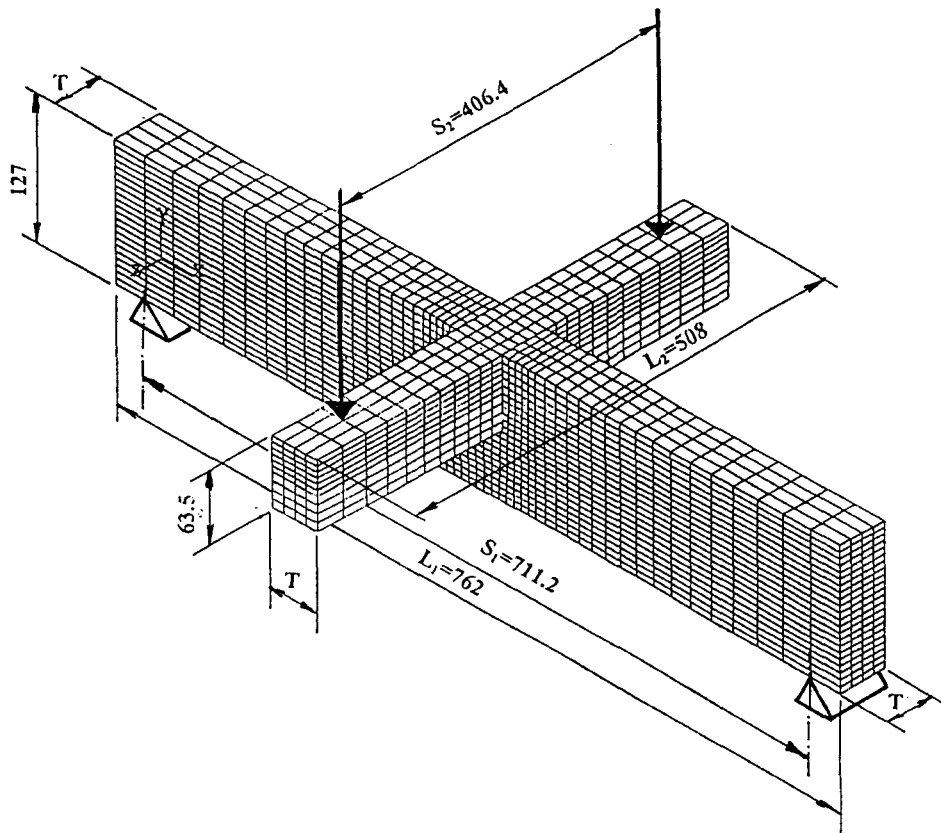
FIG. 2. Schematic and dimensions of the test specimens with the superimposed FEM mesh.

4. To experimentally validate the model.

The preliminary investigation, completed to date, was aimed at investigating the stress and deformation behavior of the proposed joint configuration. The analytical and experimental works focused on the behavior of the smallest unit of the system (i.e., cross-halved joint) under concentrated and distributed loads. Figure 2 shows this unit of the system, which was the concern of the present analysis.

This paper describes the finite element model development and predictions of stress and deformation responses of the joint under concentrated and distributed load by analytical solutions. Furthermore, the experimental work conducted and the validation of the model are discussed, along with indications for further research.

DEVELOPMENT OF THE FINITE ELEMENT MODEL

The finite element method (FEM) is one of the most important engineering achievements of the 20th century. It was first introduced in the aircraft industry and later rapidly gained acceptance and applications in other fields of applied mechanics. The finite element method is well developed, and the interested reader is referred to established textbooks on the topic for detailed discussion of the approach (e.g., Zienkiewicz 1984; Bathe 1986).

General approach

The investigated cross-halved joint represented a typical discontinuous or contact problem. Generally, such problems can be analyzed using the Hellinger-Reisner's function (Bathe 1986). This approach is based on the
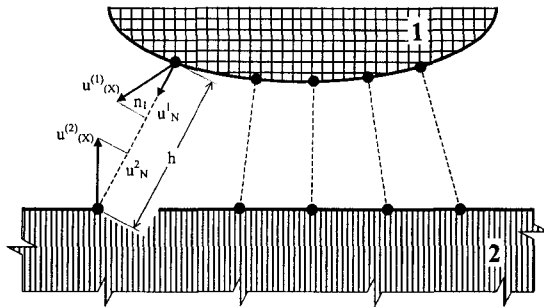
FIG. 3. Solution of the contact problem by the finite element method. Legend described in text.

TABLE 1. *Discretization of the proposed joint for FEM.*

Structural element	Number of finite elements	Number of nodal points
Primary beam	4,212	5,638
Load transferring elements	1,000	1,472
Contacting surfaces	660	—
Nodal constraints	—	107
Degree of freedom	21,223	

modification of the potential energy function where a penalty factor is added to the Lagrange multiplier term as follows:

$$L(u_i) = \Pi_p(u_i) - \int_{A_c} \left(p_i d_i(u_i) - \frac{1}{2\epsilon} p_i p_i \right) dA$$

(1)

where:

$L(u_i)$ = Hellinger-Reisner's function;
$\Pi_p(u_i)$ = total potential energy function;
A_c = contacting domain;
p_i = normal, contact stress;
d_i = gap distance;
ϵ = penalty factor.

During the iterative solution of Eq. (1), the relative positions of the two contacting, elastic bodies are computed by identifying mutually corresponding contact points at the contacting domains. These point-pairs are usually referred to as contact elements or pseudo elements. Figure 3 shows the principle of the calculation where *1* is the basic domain and *2* is the target domain. The corresponding point-pairs are identified by selecting arbitrarily one point at the basic domain, and the direction normal (n^1) from this point will intersect its pair at the boundary of the target domain. The distance between the points is given as follows:

$$d = u^1_N - u^2_N + h$$

(2)

where u^1_N and u^2_N are displacements of the points in the direction of n^1 and h is the initial gap. This distance indicates the contact or gap

development between the bodies as a result of deformations that are imposed by external loading. If $d > 0$, then there is a gap and the contact pressure, $p = 0$. On the other hand, if $d = 0$, the contact is existing and the pressure, $p \geq 0$. The commercial software used (Ansys Inc. 1998) had the capability to analyze such a discontinuous problem.

Model specifications

The performance analysis of the joint was approached as a three-dimensional, linearly elastic structural analysis modified for contact and frictional connections. We assumed geometrical linearity, i.e., only small displacements and deformations were considered upon loading.

For geometric discretization, we used an 8-node, anisotropic, rectangular solid element. The developed mesh had smaller sized finite elements near the notches for better accuracy as shown in Fig. 2. Table 1 summarizes the features of the geometrical discretization.

The primary load-bearing element was modeled as a simply supported beam that had side roller supports at the ends to prevent horizontal buckling. This resulted in 107 nodal constraints in the model. Considerations that governed the selection of load boundary conditions were: a.) the deformation of the primary beam should remain within the linear elastic region; b.) measurable deflection should be achieved for model validation; c.) the stresses in the load-transferring element should not exceed the strength values; and d.) approximately the same stress level should be generated for both composites by both loading types. Preliminary calculations, based on basic

TABLE 2. *Relationship between the global and material coordinate systems.*

Global coordinate system	Orthotropic material coordinate system	
	Primary Beam	Load-transferring element
X	L	R
Y	T	T
Z	R	L

mechanics, indicated that the following design loads would satisfy the above requirements. For both composites, two concentrated forces (406 mm apart), 3.0 kN of each were applied on the load-transferring element as shown on Fig. 2. The distributed design loads were set to 0.7 N/mm² and 0.8 N/mm² for LVL and LSL, respectively.

Based on the properties of raw materials, an orthotropic material model was incorporated. Table 3 contains the 12 elastic constants that were used to formulate the material model. The longitudinal axis of the finite elements were aligned parallel to the longitudinal (L) direction in the principal material coordinate system. Figure 4 shows the interpretation of the principal material coordinates of the composites. Note that the traditional notation, longitudinal (L), tangential (T), and radial (R)

represent the real anatomical directions of the constituents of LVL. However, in the case of LSL, these subscripts serve for identification only. Because of the material orthotropy, the elastic constants of the primary load-bearing element and the load-transferring element are different relative to the global coordinate system of the analysis. Table 2 describes the relationship between these coordinate systems.

Numerical analyses included the computation of displacement's domain and stress tensor's domain under fixed loading. Because the contact problem had physical non-linearity, the computation of the displacement within the domain required the solution of a non-linear equation system. The solution used the Newton-Raphson method (Segerlind, 1961) with 100 iterations. The convergence analysis was based on the criteria of unbalanced forces with 0.05 specific value. All finite element analyses were performed using ANSYS R5.3 software (Ansys Inc. 1998).

The analysis resulted in three-dimensional, color-coded stress distribution diagrams including normal and shear stresses. Furthermore, the model provided the spatial deformations (displacements) of the joint elements under specified loading.

TABLE 3. *Experimentally determined and estimated properties of LVL and LSL.*

Material properties	LVL			LSL		
	n[1]	$\bar{x}$	COV (%)	n	$\bar{x}$	COV (%)
E_L (GPa)	15	13.8	7.2	15	14.7	23
E_T (GPa)[2]	—	0.70	—	—	0.90	—
E_R (GPa)[2]	—	0.69	—	—	1.50	—
G_{LT} (GPa)	12	1.4	28.3	12	1.86	73
G_{LR} (GPa)	12	0.72	18.5	12	0.45	24
G_{RT} (GPa)[2]	—	0.04	—	—	0.08	—
MOR (MPa)	15	55.1	4.5	15	62.0	7.3
τ_{LR} (MPa)	45	7.04	7.0	45	12.60	14
τ_{LT} (MPa)	45	7.00	11.8	45	7.50	10.5
Poisson's ratios[2]	$\nu_{LT} = 0.40$	$\nu_{LR} = 0.32$	$\nu_{RT} = 0.32$	$\nu_{LT} = 0.38$	$\nu_{LR} = 0.50$	$\nu_{RT} = 0.83$
	$\nu_{TL} = 0.02$	$\nu_{RL} = 0.02$	$\nu_{TR} = 0.33$	$\nu_{TL} = 0.02$	$\nu_{RL} = 0.05$	$\nu_{TR} = 0.49$
Friction coefficients[3]		$\mu_s = 0.40$			$\mu_s = 0.55$	
		$\mu_k = 0.21$			$\mu_k = 0.27$	

[1] Sample size.
[2] Estimated or literature values.
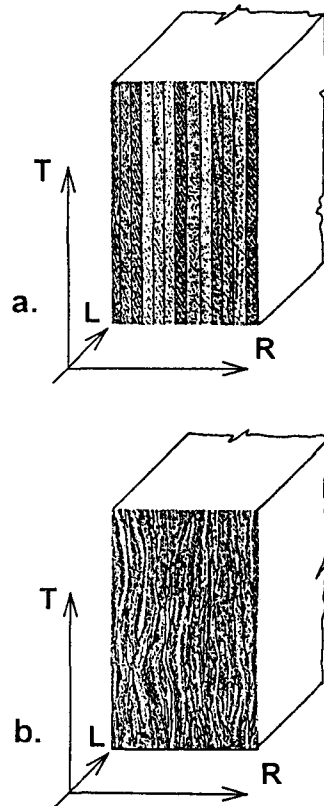[3] s, k = static and kinetic friction, respectively.

FIG. 4.   Interpretation of the material coordinate system. a.—Laminated veneer lumber (LVL); b.—Laminated strand lumber (LSL).

MATERIALS AND METHODS

Joints were manufactured from yellow-poplar (*Liriodendron tulipifera*) laminated veneer lumber (LVL) and aspen (*Populus tremuloides*) laminated strand lumber (LSL) with 44- and 38-mm thickness, respectively. Tests of required material properties included E_L, MOR, shear strength (τ), and friction coefficients (μ) determinations. Whenever possible, testing procedures followed the specifications of the relevant ASTM standards (1996) except for moduli of rigidity (G_{LT}, G_{LR}) determination. These properties were established using the single span bending method described by the European (EN 408) standard. Other elastic constants such as Poisson's rations, G_{RT}, E_R, and E_T were estimated using literature values. Calculations were based on known ratios and

symmetry requirements for orthotropic materials (Bodig and Jayne 1982; Wood Handbook 1996).

Six cross-halved joints, proposed in the lattice structure, were manufactured from each type of material. Figure 2 shows the size and configuration of these test structures. The critical feature of the joint was the tightness at the cross-halved notches. Special dado blades were used to provide precision machining. All test joints and specimens for property determination were kept in an environmental chamber set to 20°C and 45% relative humidity. This resulted in approximately 8–9% moisture content and prevented any thickness swelling after joint machining.

The solution of contact problem, included in the model, required friction coefficients of the composites. The lack of available literature data on friction coefficients of such products initiated a side study investigating the direction-dependent friction coefficients of LVL and LSL. Furthermore, the effect of contact pressure on the magnitude of friction coefficients was also examined. The details of the apparatus, testing procedure, results, and conclusions of this side study have been published in a separate paper (Bejo et al. 2000).

For experimental validation of the model, predicted and measured load displacement data were compared upon loading with concentrated and distributed loads. Test structures were loaded as simply supported beams in an MTS universal servohydraulic testing machine equipped with a 20 kN load cell. The machine operated under displacement control. The speed of testing was 2.5 mm/min. Support and load applications agreed with the specifications of the ASTM standard (Fig. 5a). Deflections were measured at two points, at both sides along the longitudinal symmetry axis of the primary load-supporting element using digital dial-gauges that had 0.01-mm accuracy. Specimens under concentrated load were tested until failure. Failure mode analysis followed.

One of the challenges of our experimental technique was the application of increasing
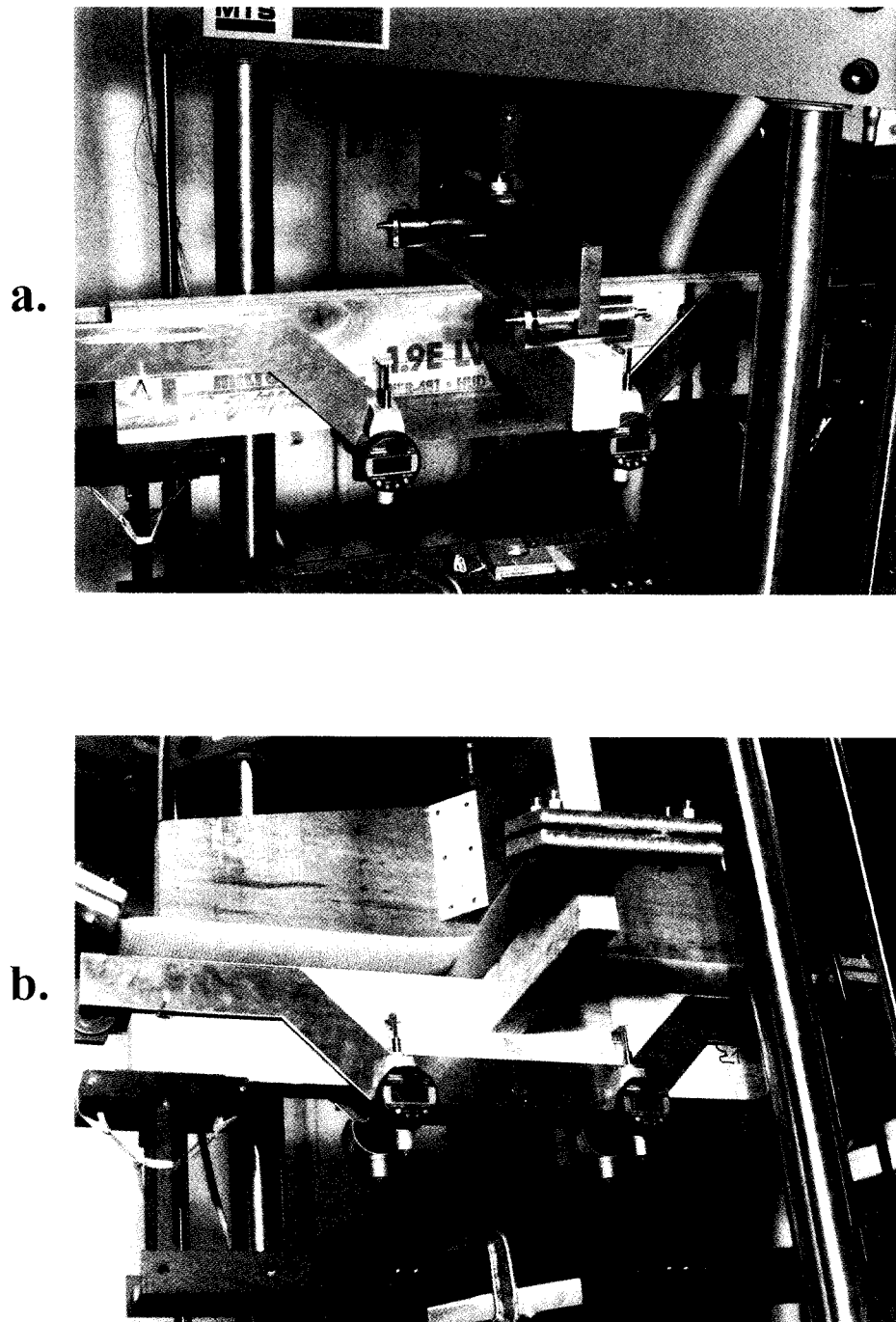
FIG. 5.   The experimental setup for model validation. a.—LVL under concentrated load; b.—LSL under distributed load.

distributed loads. We solved this problem using fire hoses partially filled with water. The hoses were placed cross-wise on the top edges of the joints. A rigid load applicator converted the concentrated force into pressure uniformly distributed on the edge surfaces of the structures (Fig. 5b).

RESULTS AND DISCUSSION

Material properties

Table 3 contains the basic statistics of the experimental test results and the values of selected properties that were used as input data of the model. In general, the measured strength and stiffness of the two types of composites were comparable. LSL, however, had higher variations in both elastic and strength properties. This fact may be explained by the more homogenous structure of LVL. On the other hand, the apparent stochastic nature of mat formation in the LSL manufacturing process creates significant in-plane density variations. Within a board, micro-voids, high and low density regions can randomly occur that may increase the variability of the evaluated engineering properties. Furthermore, LSL had a high degree of orthotropy regarding shear strength. The 12.6 MPa shear strength in the LR plane (i.e., edgewise application) compared to the strength values of LVL indicates the superiority of this product when shear is the critical design factor.

Validation of the model

The validity of the finite element model developed for the study was confirmed by comparing predicted deflections with measured ones. For both types of composites, both concentrated and distributed loads were applied within the assumed linear elastic region of the primary load-carrying element. Figures 6 and 7 compare the theoretical and actual load-deflection behavior of the joints by material and loading types.

Experimental and predicted deflections of LVL joints under concentrated load agreed perfectly (Fig. 6a). This result indicates that
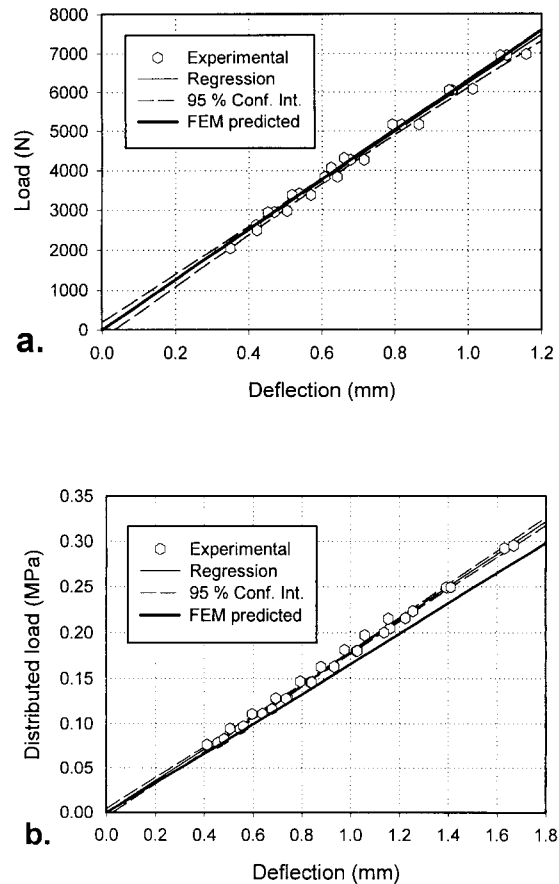

FIG. 6.   FEM predicted and experimental load-deflection behavior of the LVL joints. a.—Under concentrated load; b.—Under distributed load.

the elastic constants selected for the material are close to reality, the model is not seriously flawed, and the resolution of the FEM mesh is adequate. Under distributed load, however, the model slightly underpredicted the vertical stiffness of the joints at increased deflection as shown in Fig. 6b. This can be explained by the less controlled load application during the experiments. The different stiffness of the load applicator compared to the flexibility of the joint's elements coupled with some friction between the fire hose and the surface may have resulted in uneven pressure. If the pressure is higher near the supports, the displacement of the elastic curve may be seriously affected.

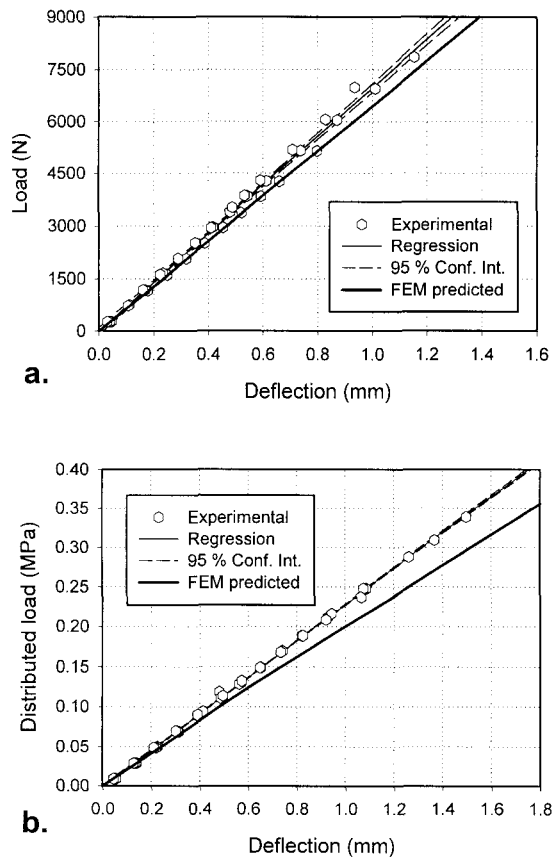The observed average deflection of LSL

Fig. 7.   FEM predicted and experimental load-deflection behavior of the LSL joints. a.—Under concentrated load; b.—Under distributed load.

samples was smaller than the model predicted. This can be attributed to the higher variability of elastic constants. Figure 7a demonstrates this fact by the different slopes of LSL joints under concentrated load. The high spread of E_L and G_{LT}, that govern the vertical deflection, did not promise excellent agreement. Similar to that of LVL, underprediction was observed for LSL joints under distributed loads. The deviation of experimental and predicted load-displacement data is more pronounced owing to the additive effect of uncertainty in material properties and imperfections in load application.

Comparing the performance of LSL and LVL joints, both model-predicted and experimental data indicated higher stiffness of LSL

under either concentrated or distributed loads. The slightly higher average values of the critical elastic constants (i.e., E_L and G_{LT}) explain this observation (Table 3).

Analytical results

The model output included color-coded diagrams showing the bending, shear, and perpendicular-to-the plane compression stress levels and distributions. Predicted stress distribution patterns were similar regarding LSL and LVL with slight differences in stress levels. No significant changes in stress distribution were observed under distributed load compared to concentrated loading. The locations of the stress concentrations were identical with similar stress level patterns.

Figure 8 shows the predicted bending stress distribution of an LVL joint under six kN concentrated load. Detail (a) discloses that the maximum tension stress of the load-transferring element exceeded the strength value of the material (i.e., $\sigma_{bmax.}$ = 59.3 MPa > MOR = 55.1 MPa). However, no failure was observed. In fact, approximately 11 kN force caused tension failure for all the tested specimens at the top of the load-transferring elements. Because the model is based on orthotropic linear elasticity and the applied loading generated strains and stresses beyond the proportional limit, these model-predicted stress level values are invalid. The distribution pattern and the location of stress concentrations, however, provide useful insight about the performance of this element. For the primary beam, the outer fiber stress in bending was expected to take a value between 9 and 16 MPa. The calculations were based on the minimum (reduced by notch size) and maximum (full) cross sections. As shown in Fig. 8b, the FEM predicted value at the tension side (12.8 MPa) is within this interval. However, twice as much compression stress developed at the bottom of the notch. This asymmetry may be explained by further studying the interactions between the two normal stresses at the vicinity of the notch. The load-transferring element in-
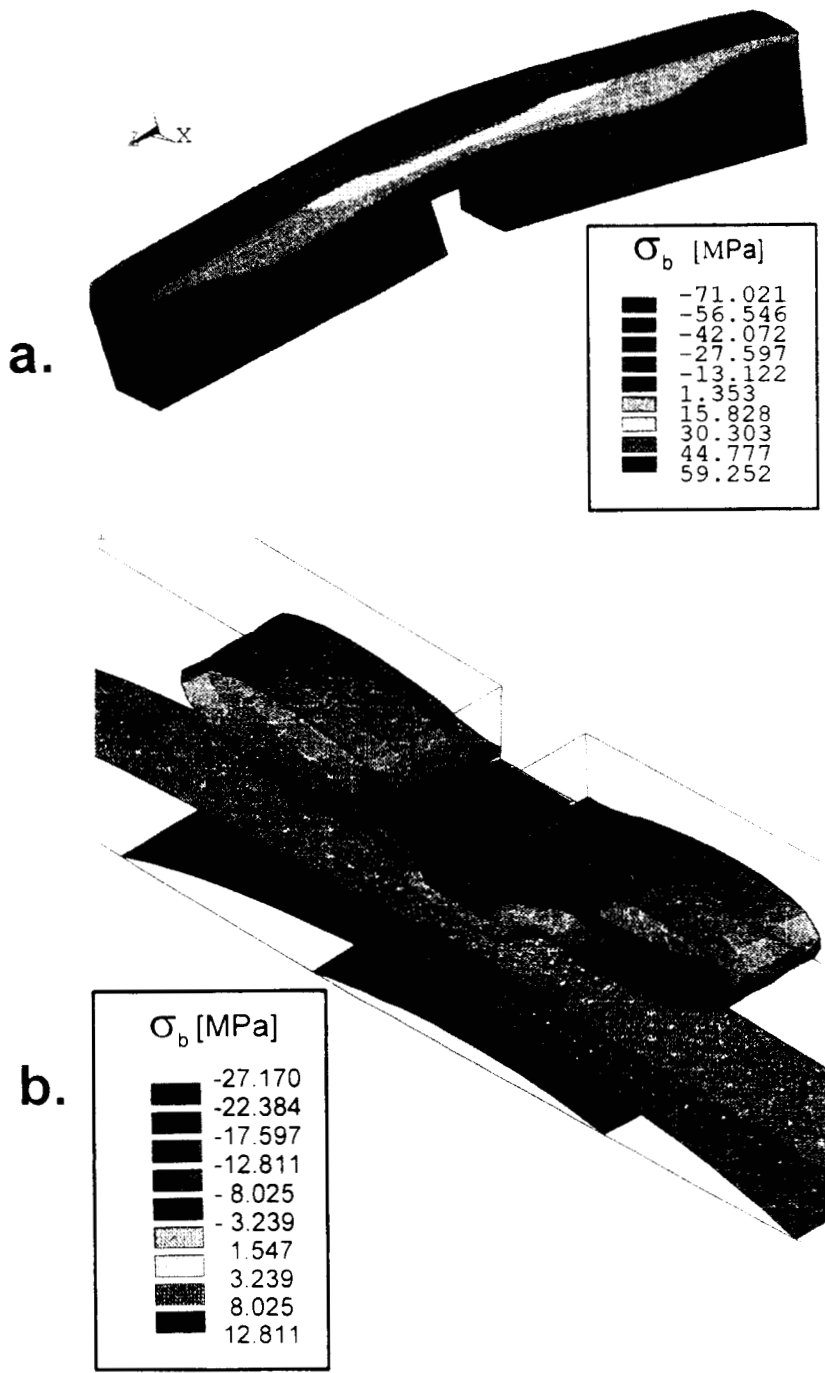
FIG. 8. Normal stress distribution due to bending in LVL joints under 6 kN concentrated design load. a.—Load-transferring element; b.—Stress distribution in the primary load-bearing element near the notch.
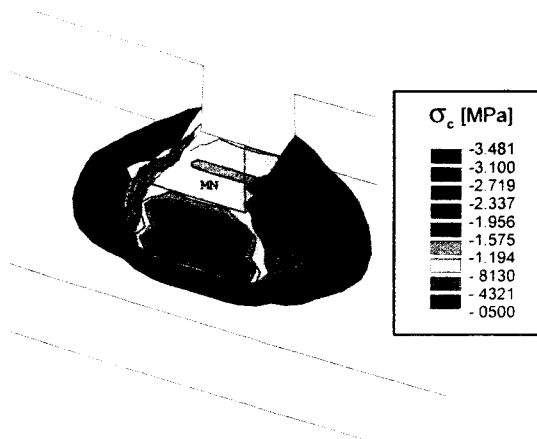
FIG. 9.   Perpendicular-to-the-plane compression stress distribution on an LVL primary load-supporting element.

duces perpendicular-to-the-plane compression on the primary beam. Figure 9 shows the distribution and levels of these stresses. The resultant constraints against the Poisson's effect in the thickness direction may contribute to the development of unique stress distribution in the primary beam. Further refined analyses are needed to better understand this phenomenon.

Maximum shear stresses were concentrated near the corners of the notches as expected. Figure 10 demonstrates the shear strength distributions in both elements. A separate analysis revealed that the friction-induced shear stresses were negligible. Thus, such stresses were excluded from further analyses. The model-predicted maximum shear stresses in the load-transferring element did not approach the experimentally determined shear strength values. This indicates that the critical stresses for designing such joints are the normal stresses. Failure modes supported the above assumption. All specimens failed in tension at the top of the load-transferring elements over the notched region.

After testing under design load, specimens were disassembled and visually inspected for unrecoverable deformations and other imperfections. No visible defects could be detected. Testing specimens up to failure, however, resulted in significant unrecoverable compression deformations of LVL primary beams as

shown in Fig. 11. LSL experienced similar penetration of the load-transferring element, albeit the unrecoverable deformations were significantly smaller in depth.

SUMMARY AND CONCLUSIONS

To further promote the application of wood-based structural composites, a finite element analysis of a cross-halved joint is presented. The joint consisted of a primary and a load-transferring element inserted into each other through rectangular notches. The FEM model, developed during this study, was based on 8-node, anisotropic, rectangular, solid elements, and was further modified to handle discontinuities. Results indicated that the developed finite element model can accurately predict the stress development and spatial displacements in such a joint. Thus, the performance of notched, structural composites can be estimated.

Both laminated veneer lumber (LVL) and laminated strand lumber (LSL) demonstrated significant potential in resisting combined stresses when notched. Although high shear stress concentrations were evident at the notches, the failure mode was always tension in the weakest cross section of the elements. The joint will be further analyzed including its response to horizontal forces. The finite element model may be further modified for predicting the performance of spatial structures, connected by the proposed jointing, under service loading conditions.
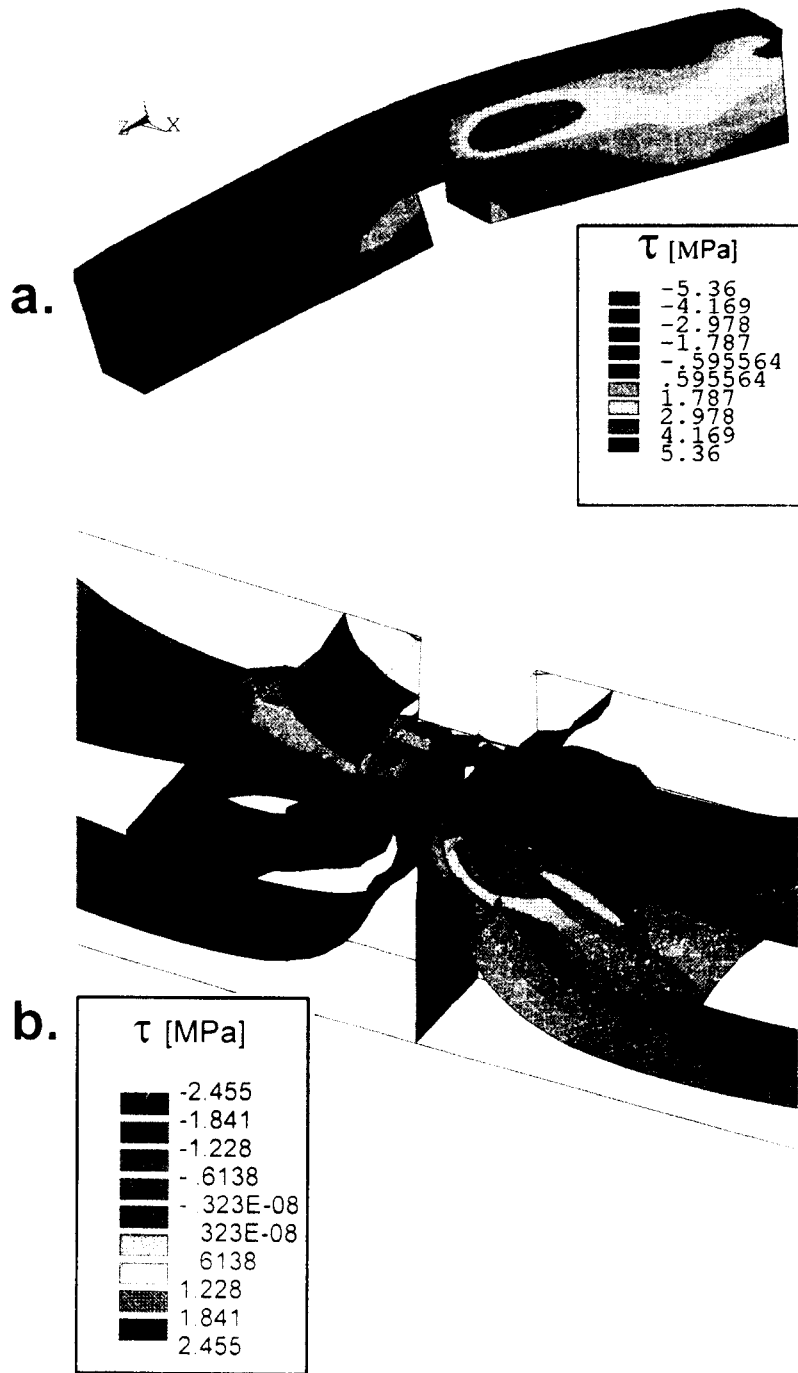
FIG. 10.   Shear stress distribution in LVL joints under 6 kN concentrated design load. a.—Load-transferring element; b.—Shear stresses distribution near the notch of the primary load-bearing element.
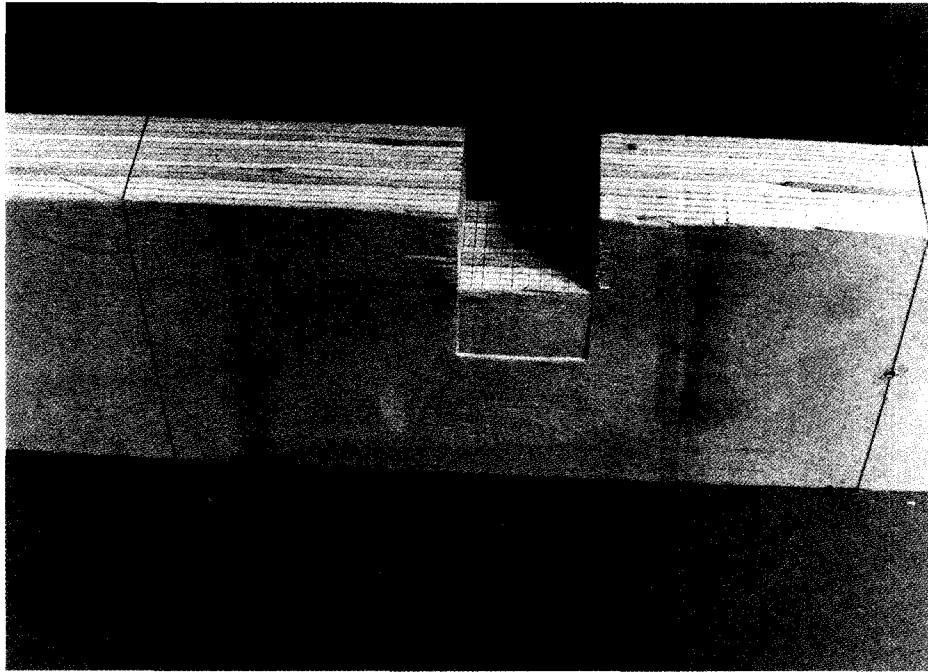
FIG. 11.   Typical unrecoverable deformation of the primary load-bearing element of an LVL specimen after tested to failure under concentrated load (~11 kN).

Forestry Experimental Station as Scientific Article No. 2751.

REFERENCES

AMERICAN SOCIETY FOR TESTING AND MATERIALS. (ASTM) 1996. Annual Book of ASTM Standards, Section 4, Construction, Volume 04.10 Wood, ASTM, West Conshohocken, PA. 645 pp.

AMERICAN SOCIETY OF CIVIL ENGINEERS. (ASCE) 1976. Latticed Structures: State-of the Art. ASCE J. Struct. Div., 102(ST11):2197–2230.

BATHE, K. J. 1986. Finite element procedures in engineering analysis. Prentice Hall Inc., Englewood Cliffs, NJ. 820 pp.

BEJO, L., E. M. LANG, AND T. FODOR. 2000. Friction coefficients of wood-based structural composites. Forest Prod. J. 50(3):39–43.

BODIG, J., AND B. A. JAYNE. 1982. Mechanics of wood and wood composites. Van Nostrand Reinhold Co., New York, NY. 712 pp.

EUROPEAN STANDARD. EN 408. 1995. Timber structures—Structural timber and glued laminated timber—Determination some physical and mechanical properties. European Committee of Standardization, Brussels, Belgium. 12 pp.

FOLIENTE, G., AND T. E. MCLAIN. 1992a. Design of notched wood beams. ASCE, J. Struct. Eng. 118(9): 2407–2420.

————, AND ————. 1992b. Strength of end-notched wooden beams: A critical fillet hoop approach. Wood Fiber Sci. 24(2):168–180.

GOODMAN, J. R., M. D. WANDERBILT, M. E. CRISWEEL, AND J. BODIG. 1974. Composite and two-way action in wood joist floor systems. Wood Science 7(1):25–32.

HOLZER, S. M., J. F. DAVALOS, AND C. Y. HUANG. 1991. A review of finite element stability investigation of spatial wood structures. B. Int. Assoc. Shell and Spatial Struct. 31(32):161–171.

KOHNKE, P., ED. 1998. Ansys User's Manual for Revision 5.0. Volume IV, Theory. Swanson Analysis Systems, Inc., Huston, PA.

LI, H., AND L. C. SCHMIDT. 1997. Posttensioned and shaped hypar space trusses. ASCE J. Struct. Eng., 123(2):130–137.

MURPHY, J. F. 1986. Strength and stiffness reduction of large notched beams. ASCE J. Struct. Eng., 112(9): 1989–2000.

SEGERLIND, L. J. 1961. Applied finite element analysis. 2nd Edition. John Wiley and Sons, New York, NY. 427 pp.

STEIDA, C. K. A. 1966. Stress concentrations around holes and notches and their effect on the strength of wood beams. J. Materials, 1(3):560–582.

SUZUKI, T., T. OGAWA, Y. FUKUOKA, T. FUKASAWA, AND S.

MOTUYU. 1994. Structural Properties of Woven Lattice Shell. International Conference on Spatial Structures: Heritage, Present and Future. 1994 Tokyo, Japan. Vol. 1.

TAKASHIMA, T. 1993. Numerical Simulation of Elastic-plastic Buckling Behavior of a Reticular Dome. Fourth International Conference of on Space Structures. Guilford, UK. Vol. 2. 1314 pp.

WOOD HANDBOOK: WOOD AS AN ENGINEERING MATERIAL 1996. USDA Handbook No. 72., U.S. Government Printing Office, Washington, DC 712 pp.

YAMADA, S. 1989. On the Effect of Joint Flexibility and Loading Conditions on the Buckling Characteristics of Single Layer Latticed Domes. International IASS Symposium 1989, Madrid, Spain. Vol. 4.

ZALPH, B. L., AND T. E. McLAIN. 1992. Strength of wood beams with filleted interior notches: A new model. Wood Fiber Sci., 24(2):204–215.

ZIENKIEWICZ, O. C., ED. 1984. The finite element method. McGraw Hill, New York, NY.